

RESEARCH PAPER

Broadband MIMO antenna for HiperLAN/2, WLAN, and WiMAX applications with high isolation

RAEFAT JALILA EL BAKOUCHI¹, MARC BRUNET², TCHANGUIZ RAZBAN² AND ABDELILAH GHAMMAZ¹

This paper presents a multiple-input and multiple-output dual-element planar inverted-F antenna (PIFA) array for broadband operation covering the High Performance radio Local Area Network/2 (5.2 GHz/5.6 GHz), Wireless Local Area Network (5.2 GHz/5.8 GHz), and the Worldwide Interoperability for Microwave Access (5.5 GHz) bands for the compact wireless communication devices. The antenna dimension is reduced substantially with a miniature ground plane. The PIFA array provides a large bandwidth (670 MHz) and a high isolation between its ports less than -26 dB. The proposed antenna has been analyzed and designed with Ansoft HFSS v.11. Then a prototype was fabricated and tested for its performance in terms of bandwidth, S-parameters, and radiation pattern. A parametric study is made to analyze the effect of different PIFA parameters on the operating frequency and the S-parameters. The diversity performances are evaluated using computer simulation technology microwave studio (CSTMWS). The broadband performance and the high isolation are achieved in both simulation and measurement.

Keywords: Broadband antenna, Multiple Input Multiple Output (MIMO), High Isolation, HiperLAN/2, WLAN, WiMAX

Received 21 June 2014; Revised 8 December 2014; Accepted 15 December 2014; first published online 9 January 2015

I. INTRODUCTION

Owing to their ability to combat multipath fading and to deliver higher data rates; multiple-input and multiple-output (MIMO) systems become a well-known technique to enhance the performance of wireless communication systems [1]. However; in a MIMO system, it is necessary to use several transmitter and receiver antennas at each end of the radio link, the signals received should be uncorrelated to achieve a high capacity [2–6]. These antennas must be capable of receiving signals independently, even they are closely spaced.

However, it is usually difficult to implement multiple antennas within small communication devices such as mobiles handsets. That latter happened to increase the mutual coupling and results high correlation coefficients. A good isolation between antennas and a good radiation patterns are required to obtain a better MIMO channel capacity.

Owing to its high performance, the planar inverted-F antenna (PIFA) is used as internal antenna for mobile communication devices. Some techniques must be applied to increase the isolation between the antenna elements, such as using a defected ground plane [7], inserting a small ground plane between PIFA and the mobile circuit board [8, 9] and

maintaining the distance between antenna elements, as the critical parameter affecting the mutual coupling, at least equal to a half wavelength [8–10]. Thus, other techniques to make PIFA broadband such as inserting slots [11] and a parasitic element [12] can be applied. Otherwise, these techniques as well as the use of capacitive load [13] and shaped strip [14] are used to achieve multiband performance [15–17].

A broadband dual-element PIFA antenna array for MIMO application is proposed. To increase the isolation between the PIFAs, a small ground plane and a parasitic element are placed between the radiating plate and the PCB. They are used also to widen the bandwidth. The antenna operates at the High Performance radio Local Area Network/2 (HiperLAN/2) (5.15–5.35 GHz, 5.47–5.725 GHz), the Wireless Local Area Network (WLAN) (5.15–5.35 GHz, 5.725–5.825 GHz), and the Worldwide Interoperability for Microwave Access (WiMAX) (5.25–5.85 GHz) frequency bands. Parametric investigation of the antenna is carried out to analyze the effect of the shape parameters on the operating frequency, the return loss as well as the isolation between the two PIFAs. The diversity characteristics and MIMO performance are evaluated in terms of envelope correlation coefficient (ECC) and diversity gain. The antenna characteristics are evaluated in both simulation and measurement.

II. ANTENNA DESIGN

Figure 1 shows the geometry of the proposed MIMO antenna array. The symmetrical back to back antenna elements are

¹Laboratory of Electrical Systems and Telecommunications, Faculty of Sciences and Technologies, Cadi Ayyad University, Avenue Abdelkarim Elkhatabi, Marrakesh 40000, P.O.BOX 549, Morocco. Phone: +212 613711690

²Electronics and Telecommunications Institute of Rennes (IETR-UMR 6164), Ecole Polytechnique of the University of Nantes France, IETR, Nantes, France

Corresponding author:

R.J. El Bakouchi

Email: jalila.elbakouchi@ced.uca.ma

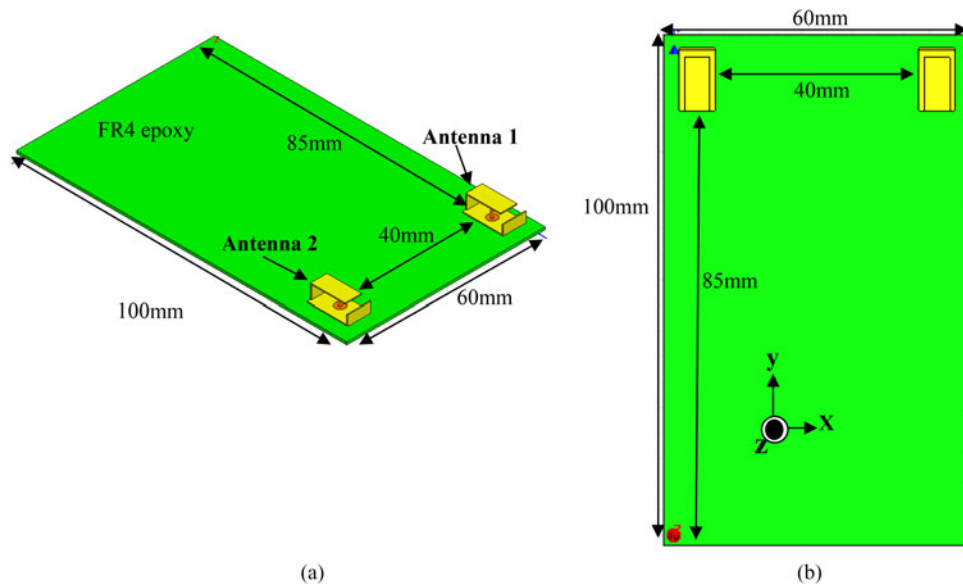


Fig. 1. Configuration of the proposed antenna: (a) 3D view and (b) top view.

referred to Antenna1 and Antenna2. They are placed 2.7 mm from top and 3 mm from side on the system circuit board (PCB) with a separation of 40 mm (more than half wavelength $\lambda = 53.95$ mm, $40\text{ mm} = 0.74\lambda$). An FR4 substrate of size $100 \times 60 \times 0.8\text{ mm}^3$ is used as a PCB ($\epsilon_r = 4.4$ and $\tan \delta = 0.018$), on which the system ground plane of size $100 \times 60\text{ mm}^2$ is printed below.

Figure 2 shows the details of the PIFA antenna element. The dimensions of the PIFA element are $WS = 5$ mm, $LT = 10.5$ mm, and $T = 0.3$ mm. And the high of the antenna (H) is equal to 4 mm as shown in Table 1.

The technique of locating a small ground plane between the PIFA and PCB [8, 9] is used in this study. It was made

by collecting a rectangular plate with dimensions of $WG = 7$ mm, $LG = 12$ mm, and $T = 0.3$ mm, to a parasitic element ($WG = 7$ mm, $HPE = 2.7$ mm, and $T = 0.3$ mm). The small ground plane (rectangular plate) between the PIFA and the FR4 substrate with a gap of 1.2 mm is used to maintain good isolation between the antenna elements. Also it completes the part of the parasitic element which consists on widen the bandwidth, minimizing the reflection losses and providing the fine tuning to cover the entire band of operation. Plus to maintaining the high isolation, the small ground plane contributes on the width of the bandwidth to cover properly HiperLAN/2, WLAN, and WiMAX frequency bands.

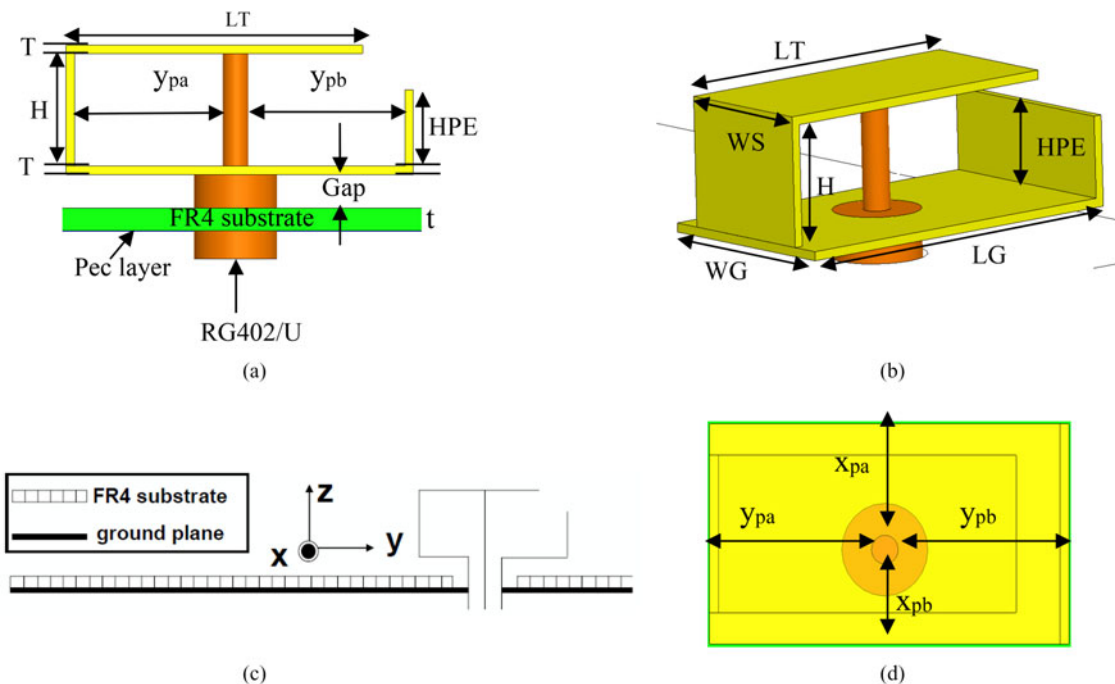


Fig. 2. View of the single antenna element of the proposed MIMO antenna: (a) profile view, (b) 3D view, (c) front view, and (d) top view.

Table 1. Optimized values of antenna array parameters.

Parameter	Dimension (mm)
<i>LT</i>	10.5
<i>WS</i>	5
<i>WG</i>	7
<i>LG</i>	12
<i>H</i>	4
<i>HPE</i>	2.7
<i>T</i>	0.3
<i>t</i>	0.8
<i>Gap</i>	1.2
<i>x_{pa}</i>	3.544
<i>x_{pb}</i>	2.544
<i>y_{pa}</i>	5.544
<i>y_{pb}</i>	5.544

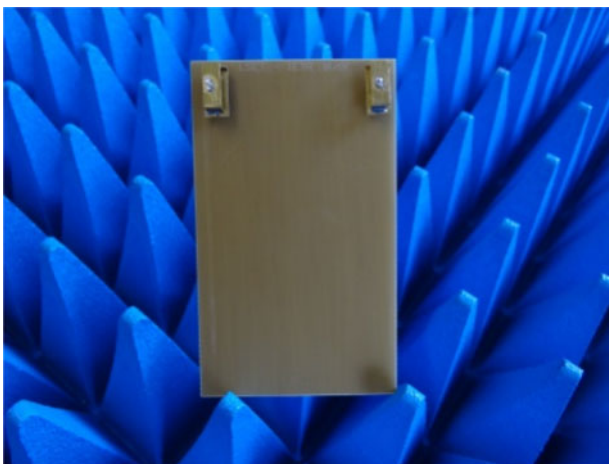
The thickness of the copper sheet is 0.3 mm. The antenna is fed by the 50 ohm RG402/U (1673A) coaxial cable ($d = 0.912$ mm, $D = 2.95$ mm, and $\epsilon = 2.1$).

III. RESULTS AND DISCUSSION

A) The S-parameters

A prototype of the proposed antenna, as shown in Fig. 3, was fabricated in the Electronics and Telecommunications Institute of Rennes (IETR), Ecole Polytechnique of the University of Nantes, France. A ZVA24R&S vector network analyzer was used to measure the S-parameters.

The S-parameters were measured and compared to the simulation results in Fig. 4. The simulations are performed originally in Ansoft's High Frequency Structure Simulator (Ansoft HFSSTM v.11), which is based on the finite-element method. The S-parameters simulated using CST MWS will be used to evaluate the diversity performance in section E. The simulated return losses of both PIFAs are identical due to the symmetric configuration. The measured return loss of Antenna 1 is slightly different from that of Antenna 2. This is due to the imperfection in the fabrication of two PIFAs. The measured resonant frequency of Antenna 1 is at 5.485 GHz, which is 0.075 GHz lower than the simulated

**Fig. 3.** The prototype of the proposed MIMO system.

one (5.56 GHz). The measured resonant frequency of Antenna 2 is at 5.51 GHz, which is 0.05 GHz lower than the simulated one (5.56 GHz). The measured bandwidths at -10 dB of Antenna 1 and 2, as shown in Table 2, span more than 644 MHz (narrower than the simulated one (879 MHz)), where the lower resonant frequency is 5.18 GHz (less than the simulated one (5.19 GHz)) and the upper resonant frequency is more than 5.825 GHz (less than the simulated one (6.07 GHz)). These bandwidths have covered the band of WLAN (5.2 GHz/5.8 GHz), WiMAX (5.5 GHz) as well as HiperLAN/2 (5.2 GHz/5.6 GHz).

It is also shown in Fig. 4 where a high isolation better than 16.45 dB in simulation and better than 26 dB can be achieved in measurement. This is due to the space between the PIFAs that is more than the half wavelength (0.74λ) as well as the use of the small ground plane between the PIFA and the FR4 substrate.

Both simulated and measured results confirm the broadband performance of the antenna, its low return loss, the high isolation between its elements.

For comparison, a dual-element conventional PIFA with same height (H), width (WS), same location and same size of PCB as those of the broadband MIMO system was investigated. The length is 8 mm greater than that of the proposed MIMO antenna to achieve an operation in the 5 GHz band. The small ground plane and the parasitic element are removed from the model and the PCB acts as the ground plane. The S-parameters of the conventional PIFA array are shown in Figure 5.

At -10 dB, the bandwidth is equal to 580 MHz, which is 90 MHz narrower than the measured bandwidth (670 MHz) and 299 MHz narrower than the simulated one (879 MHz). The antenna covers just the WLAN frequency band (5.725–5.825 GHz). HiperLAN/2 (5.15–5.35 GHz, 5.47–5.725 GHz), WLAN (5.15–5.35 GHz), and WiMAX (5.25–5.85 GHz) frequency bands are not covering.

The isolation between the two elements is -22 dB, which is 4 dB worse than the measured one of the proposed broadband MIMO antenna array. This isolation is due to the space between the PIFAs that is more than the half wavelength (0.74λ).

For this antenna design, the small ground plane and the parasitic element are an essential component because they widen the bandwidth to cover the entire band of operation (5 GHz band), maintain a high isolation (-26 dB) between the antenna elements and reduce substantially the antenna dimensions.

B) Parametric study of the S-parameters

In this section, a parametric investigation of some critical dimensions of the antenna configuration is carried out to analyze the effect of the parameters on the operating frequency bands, the return loss and the isolation between the two antennas. The study has been performed using HFSS.

Figure 6 shows the effect of probe feed position y_{pa} from the shorting plate on the S-parameters when keeping the parameter x_{pa} fixed at 4 mm. It is observed that with the increase of the distance y_{pa} the resonant frequency increases with minimization of the reflection S-parameter value. The optimized value for y_{pa} is obtained to be 6 mm.

We can say that the positions of the probe feed are very sensitive to the antenna operating bands (WLAN, WiMAX, and HiperLAN/2).

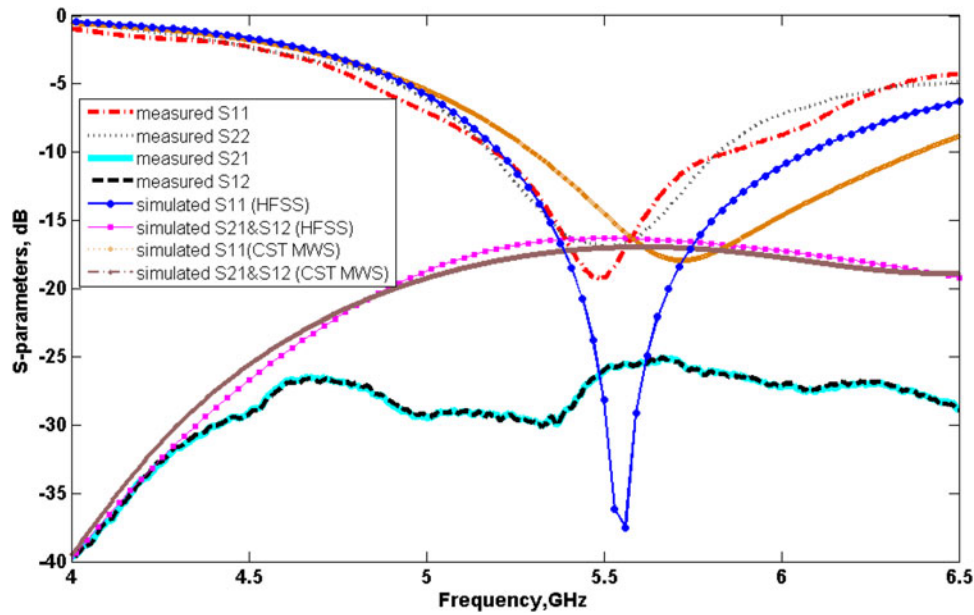


Fig. 4. Measured and simulated S-parameters of the MIMO antenna array.

Figure 7 shows the performance of the MIMO antenna array with different width of the shorting plate (WS). It is observed that when the width increases the resonant frequency increases from 5.1 to 5.56 GHz with minimization of the reflection losses and the bandwidth widens. We get WLAN, WiMAX, and HiperLAN/2 bands properly. The isolation remains constant in all the width values. It is still below -16.34 dB. The optimized length of the shorting plate is 5 mm.

Figure 8 shows the effect of the high of parasitic element (HPE) on the simulated S-parameters. From 1 to 2.5 mm, the bandwidth widens but the 5 GHz band is not covering and the reflection losses are maximizing. For 3, 3.5, and 4 mm, the bandwidth widens and covers the entire bands of operation without sacrificing the reflection losses. The optimized value is 3 mm.

Figure 9 shows the effect of the length of the small ground plane (LG) on the simulated S-parameters. The small ground plane is used to maintain good isolation between the antenna elements. It can be seen that up to 10 mm, the bandwidth widens to provide the fine tuning to cover the 5 GHz bands of operation with good minimization of reflection losses and isolation equal to 16.45 dB. The small ground plane completes the part of the parasitic element to cover properly HiperLAN/2, WLAN, and WiMAX frequency bands. The optimized value of the length of the small ground plane is 12 mm.

Table 2. Measured and simulated lower, upper frequency, and bandwidth at -10 dB for Antennas 1 and 2.

	fl (GHz)	fu (GHz)	Bandwidth (MHz)
Simulated antennas 1 and 2 (HFSS)	5.196	6.075	879
Simulated antennas 1 and 2 (CST MWS)	5.29	6.36	1070
Measured antenna 1	5.19	5.86	670
Measured antenna 2	5.18	5.825	645

Figure 10 shows the performance of the proposed MIMO antenna array with different gap between the small ground plane and the PCB. It is observed that when the gap increases the resonant frequency reduces from 5.5 to 4.9 GHz and we are not getting WLAN, WiMAX, and HiperLAN/2 bands properly. But with decrease of the gap value we get the operating bands properly with minimized reflection losses. The isolation remains constant in all the gap values. It is still below -16.34 dB. The optimized value is 1.2 mm because it provides the fine tuning to cover the entire band of operation.

Each time, one of these parameters is kept fixed, while the other one is optimized. The optimized values are shown in Table 1.

C) Current distribution

To further investigate the good isolation between the antenna elements, HFSS was used to generate images of the surface current distributions when one antenna is excited while the other is terminated with a matched load. Figure 11 illustrates the current distributions at the resonant frequency (5.56 GHz). It is observed that most of the currents are confined in the location of the excited antenna, allowing the two antennas to function independently. The small ground plane between the PIFA and the PCB play a significant role in providing the high isolation preventing the current flow on the excited PIFA to reach the PCB and the other antenna.

D) Radiation pattern

The radiation patterns of the prototype PIFA were measured, inside an anechoic chamber with the transmitting field provided by 2–18 GHz dual polarization quad-ridge horn antenna, when one antenna is excited while the other one is terminated with 50-ohms matched load.

Figures 12 and 13 show the measured radiation patterns at the resonant frequencies (5.485 GHz for Antenna 1 and 5.51 GHz for Antenna 2). The ripples in the measured

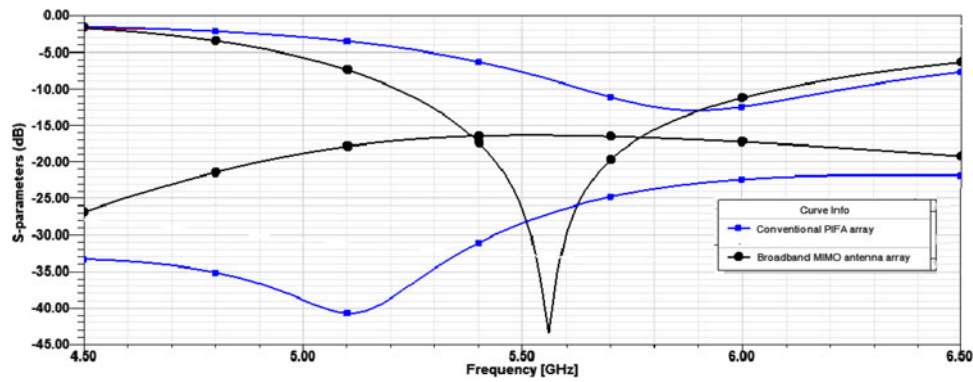


Fig. 5. Simulated S -parameters of the conventional PIFA array and the proposed MIMO antenna array.

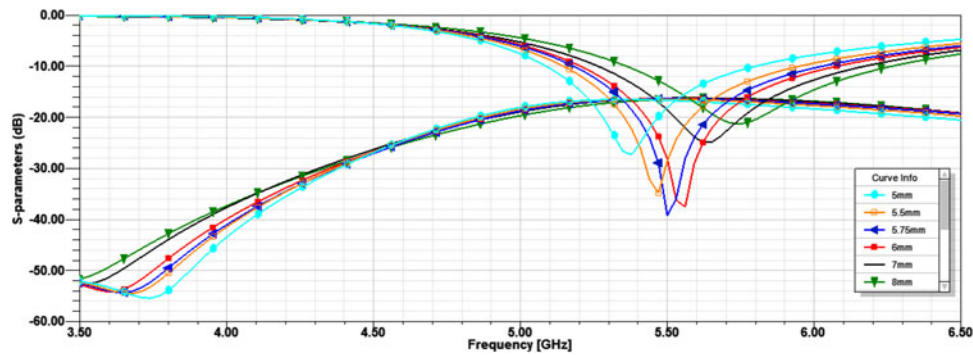


Fig. 6. Effect of the position y_{pa} of the probe feed on the S -parameters.

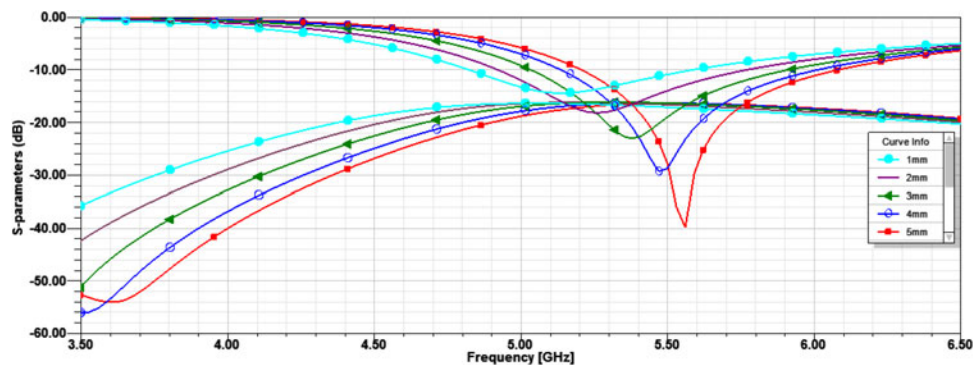


Fig. 7. Effect of the width of the shorting plate on the simulated S -parameters.

radiation patterns are due to the effect of the long and bent feeding cable used in the measurement. Because of the PCB which acts as a reflector, the power is directed toward the positive z -direction ($\theta = 0^\circ$). So the radiation patterns along the XZ and YZ -planes are measured between 270° and 90° which is the region above the PCB. In Fig. 12(a) the radiation between 270° and 360° is stronger than that between 0° and 90° owing to the Antenna 1's left place on the PCB. The inverse vision in the Fig. 13(a) observed where Antenna 2 is placed in the right corner of the PCB. The radiation patterns in Figs 12(b) and 13(b) are plotted along the YZ -plane. They are asymmetrical in the positive and negative Y -directions.

The radiation patterns in Figs 12(c) and 13(c) are measured along the XY -plane. It is noticed that the radiation patterns of Antennas 1 and 2 are complementary to each other. The

direction of maximum radiation for each pattern is tilted at about 45° around the z -axis toward the handset with respect to XY -plane. The radiation patterns of both antennas are orthogonal to each other to achieve good pattern diversity characteristics.

E) ECC and diversity gain

The ECC and diversity gain are used to evaluate the diversity characteristics and MIMO performance of the proposed antenna using CST MWS.

The ECC is used to evaluate the diversity capability of the MIMO antenna. This parameter should ideally be computed using three-dimensional (3D) radiation pattern. Computation of correlation coefficient based on radiation

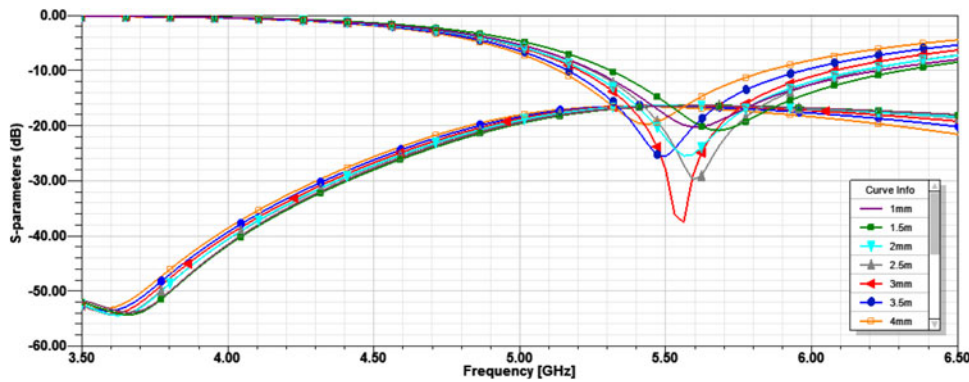


Fig. 8. Effect of the parasitic element on the simulated S-parameters.

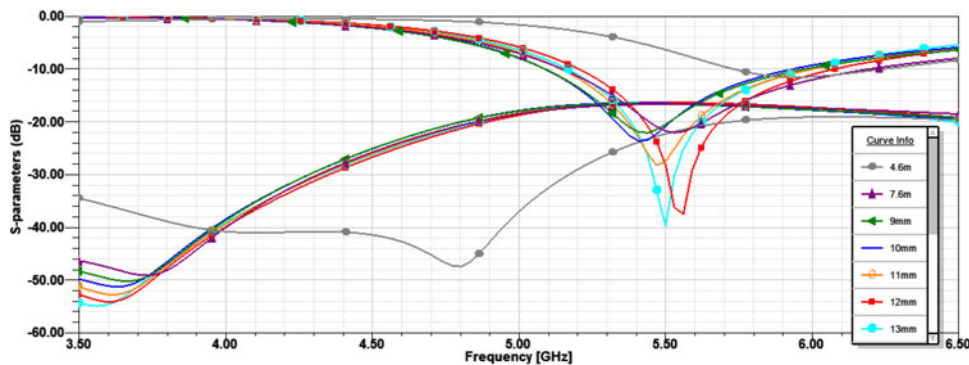


Fig. 9. Effect of the length of the small ground plane on the simulated S-parameters.

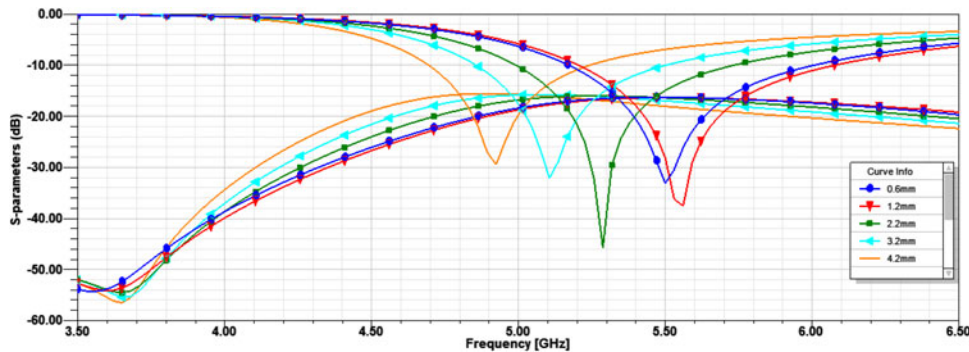


Fig. 10. Effect of the gap on the simulated S-parameters.

patterns involves integral equations, which are numerically time consuming. To make this process easier, a method for calculating the ECC from the S-parameters of the diversity antenna system has been derived in [18], i.e.

$$\rho_e = \frac{|S_{11}^* S_{12} + S_{22} S_{21}^*|^2}{(1 - |S_{11}^2 + S_{21}^2|)(1 - |S_{22}^2 + S_{12}^2|)} \quad (1)$$

Figure 14 shows the simulated results of ECC with respect to frequency. The simulated S-parameters are those obtained from CST MWS. It can be observed that the ECC values are less than 0.1 for the desired bands, which satisfy the desired diversity criteria of an ECC less than 0.5.

We will look at the relation between the correlation coefficient ρ_p and the apparent diversity gain G_{app} of a two antenna system. The following approximate formula applies.

$$G_{app} = 10^* \rho_p = \sqrt{1 - |\rho_e|^2} \quad (2)$$

where 10 dB is the maximum apparent diversity gain at the 1% probability level with selection combining, and ρ_p is an approximate expression for the correlation efficiency, i.e. the reduction in diversity gain due to correlation between the signals on the two branches. This formula is not very accurate for correlations as it is close to unity when compared with the more accurate formulas in [18]. However, if we scale

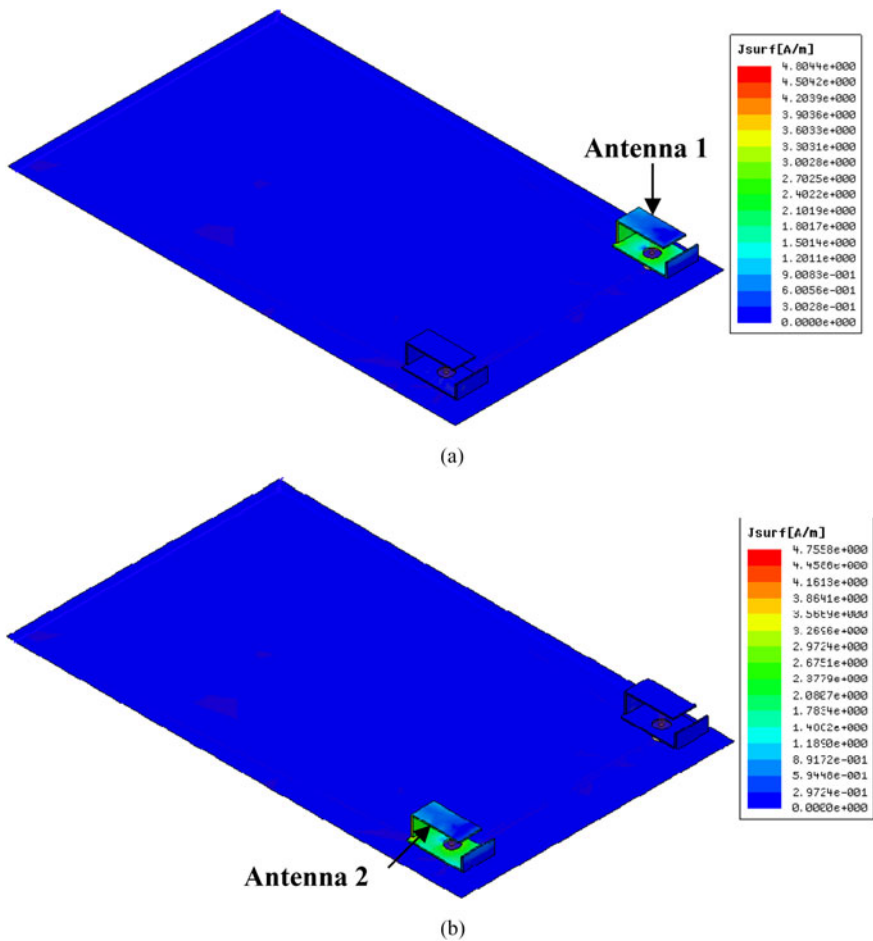


Fig. 11. Surface current distribution: (a) when the Antenna 1 is excited and Antenna 2 is matched, (b) when Antenna 2 is excited and Antenna 1 is matched.

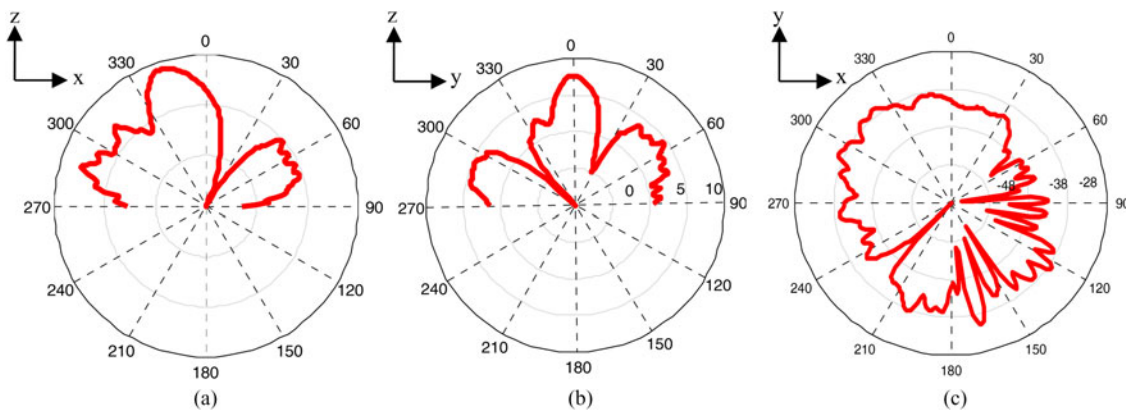


Fig. 12. Measured radiation pattern when Antenna 1 excited and Antenna 2 is terminated on (a) the XZ-plane, (b) the YZ plane, and (c) the XY plane.

ρ_p with a factor 0.99, the formula becomes,

$$\rho_e = \sqrt{1 - |0.99 * \rho_e|^2}, \tag{3}$$

which differs from the more accurate expression for the apparent diversity gain at the 1% probability level by

<0.1 dB. Figure 15 shows the variation of the diversity gain versus the frequency for the MIMO antenna system for WLAN, WiMAX, and HiperLAN/2 applications.

The ECC and diversity gain at 1% of probability level by <0.1 dB are listed in Table 3. The calculated result in Table 3 satisfy the criteria of low correlation ($\rho_e < 0.5$), and good diversity performance can be expected in practical multipath environments.

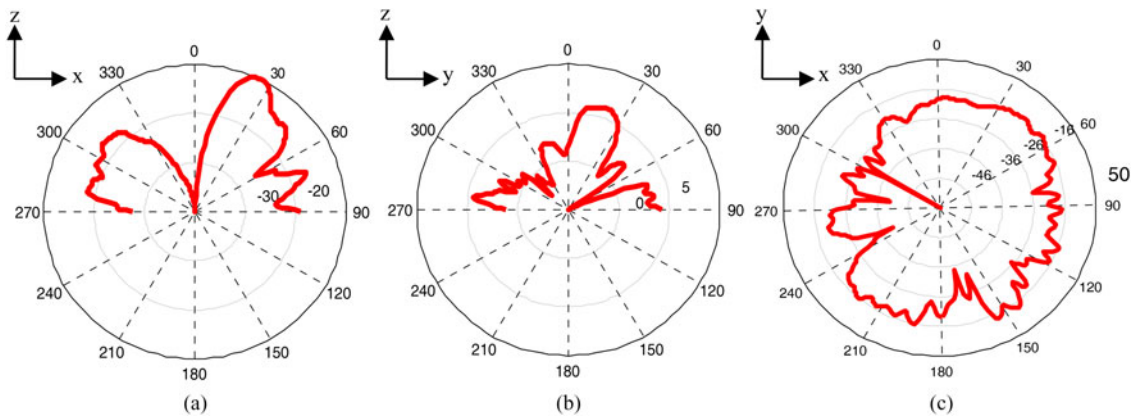


Fig. 13. Measured radiation pattern when Antenna 2 excited and Antenna 1 is terminated on (a) the XZ-plane, (b) the YZ plane, and (c) the XY plane.

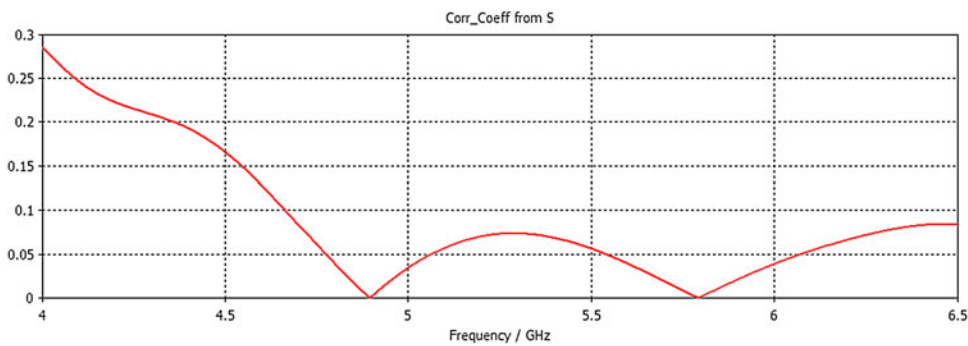


Fig. 14. The simulated ECC for the proposed MIMO antenna system.

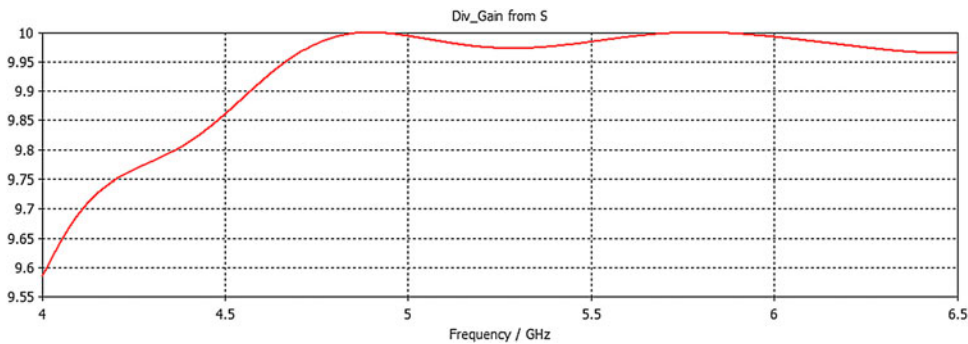


Fig. 15. The variation of the diversity gain versus the frequency for the MIMO antenna system.

Table 3. Diversity performance of MIMO antenna system.

Frequency band	ECC	Diversity gain (1%) (dB)
WLAN 5.2 GHz (5.15–5.35 GHz)	0.073	9.97
WiMAX 5.5 GHz (5.25–5.85 GHz)	0.055	9.98
HIPERLAN /2 5.6 GHz (5.47–5.725 GHz)	0.037	9.99
WLAN 5.8 GHz (5.725–5.825 GHz)	0.0019	10

IV. CONCLUSION

A MIMO antenna for WLAN (5.2 GHz/5.8 GHz), WiMAX (5.5 GHz), and HiperLAN/2 (5.2 GHz/5.6 GHz) applications

has been proposed. It provides a broad bandwidth (670 MHz) and a high isolation (better than 26 dB) between the radiating elements. Its high performances are due to inserting a small ground plane technique between the PIFA and the PCB. Parametric investigation has been proposed to analyze the effect of different PIFA parameters on the operating frequency and the S-parameters. Good radiation characteristics and diversity performance over the operating bands have been observed.

Experimental results have been done and shown a good agreement with simulation. The results of the mutual coupling and the radiation pattern allowed achieving the good diversity characteristics of the proposed MIMO antenna.

REFERENCES

- [1] Vaughan, R.G.; Andersen, J.B.: Antenna diversity in mobile communications. *IEEE Trans. Veh. Technol.*, **VT-36** (1987), 149–172.
- [2] Karaboikis, M.; Soras, C.; Tsachtsiris, G.; Makios, V.: Compact dual-polarity inverted-F antenna diversity systems for portable wireless devices. *IEEE Antennas Propag. Lett.*, **3** (2004), 9–14.
- [3] Ding, Y.; Du, Z.; Gong, K.; Feng, Z.: A novel dual-band printed diversity antenna for mobile terminals. *IEEE Trans. Antennas Propag.*, **55** (2007), 2088–2096.
- [4] Murch, R.D.; Letaief, K.B.: Antenna systems for broadband wireless access. *IEEE Commun. Mag.*, **40** (2002), 76–83.
- [5] Foschini, G.J.: Layered space-time architecture for wireless communication in a fading environment when using multi-element antennas. *J. Bell Labs Tech.*, **1** (1996), 41–59.
- [6] Wallace, J.; Jensen, M.; Swindlehurst, A.; Jeffs, B.: Experimental characterization of the MIMO wireless channel: data acquisition and analysis. *IEEE Trans. Wireless Commun.*, **2** (2003), 335–343.
- [7] Meshram, M.K.; Animeh, R.K.; Pimpale, A.T.; Nikolova, N.K.: A Novel quad-band diversity antenna for LTE and Wi-Fi applications with high isolation. *IEEE Trans. Antennas Propag.*, **60** (2012), 4360–4371.
- [8] Gao, Y.; Chen, X.; Ying, Z.; Parini, C.G.: Design and performance investigation of a dual-element pifa array at 2.5 GHz for MIMO terminal. *IEEE Trans. Antennas Propag.*, **55** (2007), 3433–3441.
- [9] Gao, Y.; Chiau, C.C.; Chen, X.; Parini, C.G.: Modified PIFA and its array for MIMO terminals. *Inst. Elect. Eng. Proc. Microw. Antennas Propag.*, **152** (2005), 253–257.
- [10] Balanis, C.A.: *Antenna Theory Analysis and Design*, 3rd ed., Wiley Inc. Hoboken, New Jersey, USA, 2005.
- [11] Shagar, A.C.; Wahidabanu, S.D.: Novel wideband slot antenna having notch-band function for 2.4 GHz WLAN and UWB applications. *Int. J. Microw. Wireless Technol.*, **3** (2011), 451–458.
- [12] Ibnyaich, S.; Ghammaz, A.; Hassani, M.M.: Planar inverted-F antenna with J-shaped slot and parasitic element for ultra-wide band application. *Int. J. Microw. Wireless Technol.*, **4** (2012), 613–621.
- [13] Sanz-Izquierdo, B.; Batchelor, J.; Langley, R.: Multiband printed PIFA antenna with ground plane capacitive resonator. *Electron. Lett.*, **40** (2004), 1391–1392.
- [14] Tseng, C.F.; Chen, Y.W.: Small pifa for ZigBee and wlan application. *Microw. Opt. Technol. Lett.*, **55** (2013), 1074–1077.
- [15] Ben Ahmed, M.; Bouhorma, M.; Elouaai, F.; Mamouni, A.: Low SAR planar antenna for multi standard cellular phones. *Eur. Phys. J. Appl. Phys.*, **53** (2011), 33604.
- [16] Panaia, P.; Luxey, C.; Jacquemod, G.; Staraj, R.; Petit, L.; Dusopt, L.: Multistandard reconfigurable pifa antenna. *Microw. Opt. Technol. Lett.*, **48** (2006), 1975–1977.
- [17] Nepa, P.; Manara, G.; Serra, A.A.; Nenna, G.: Multiband PIFA for WLAN mobile terminals. *IEEE Antennas Wireless Propag. Lett.*, **4** (2005), 349–350.
- [18] Blanch, C.; Romeu, J.; Corbella, I.: Exact representation of antenna system diversity performance from input parameter description. *Electron. Lett.*, **39** (2003), 705–707.



Raefat Jalila El Bakouchi was born in Morocco, in 1987. She received her Bachelor of sciences (3 years study after the baccalaureate) in Electrical Engineering from Cadi Ayyad University, Marrakesh Morocco, in 2008. She received her Master of Science and Technology (M.Sc. Tech. (Eng)) in Electrical Engineering, Cadi Ayyad University; Marrakesh Morocco, in 2010. She is currently working toward the Ph.D. degree at the Department of Applied Physics, Electrical Systems and Telecommunications Laboratory, Cadi Ayyad University of Marrakesh, Morocco. Her research interest includes telecommunications and antennas.



Marc Brunet Engineer in electronics at the Electronics and Telecommunications Institute of Rennes (IETR-UMR 6164), Ecole Polytechnique of the University of Nantes France, IETR, Nantes, France.



Tchanguiz Razban Haghghi Professor at the Department of Electronic and Digital Technologies, and Head of International Relations Office of Ecole Polytechnique of the University of Nantes France, IETR, Nantes, France. His research interests in the field of high frequency electronics.



Abdelilah Ghammaz received his Doctor of Electronic degree from the National Polytechnic Institute (ENSEEIH) of Toulouse, France, in 1993. In 1994 he went back to University Cadi Ayyad of Marrakech – Morocco. Since 2003, he has been a Professor at the Faculty of Sciences and technology, Marrakech, Morocco. His research interests in the field of electromagnetic compatibility and antennas.